第 24 卷第 1 期 无 机 化 学 学 报 Vol.24 No.1
2008 年 1 月 CHINESE JOURNAL OF INORGANIC CHEMISTRY 130~137

高度有序介孔氧化硅材料 SBA-15：高浓度氨基官能化及氨基及氨基团的可利用性

韦 奇*,[1] 钟振兴[1] 聂祚仁[1] 陈慧巧[1] 李群艳[1] 李从举[2]
([1]北京工业大学材料科学与工程学院,北京 100022)
([2]北京服装学院北京市服装材料研发与评价重点实验室,北京 100029)

摘要：采用简单的方法合成高浓度氨基修饰的高度有序氧化硅材料并深入研究氨基官能化材料的孔结构以及氨基的存在状态和可利用性。结果表明,氨基基团共价连接到 SBA-15 的孔表面,即使初始合成体系中的 APTES(氨丙基三乙氧基硅烷)浓度高达 30mol%时材料依然保持高度的有序性。合成体系中 APTES 浓度为 20%的样品还保持良好的介孔结构,比表面积为 680 $m^2 \cdot g^{-1}$,孔容为 0.89 $cm^3 \cdot g^{-1}$,此介孔结构中的氨基官能团对镍离子表现出很强的亲和力,Ni^{2+}的吸附量高达 1.88 $mmol \cdot g^{-1}$,相比之下未官能化的 SBA-15 对 Ni^{2+}没有吸附作用。当初始合成体系中 APTES 的浓度进一步增大到 30%时,修饰到介孔氧化硅材料的氨基含量也随之增大,但由于材料的孔隙度急剧降低,这些氨基的可利用性也降低。

关键词：氨基；介观有序度；孔结构；金属离子吸附
中图分类号：O612.4；O623.732；TB321 **文献标识码**：A **文章编号**：1001-4861(2008)01-0130-08

Highly Ordered Mesoporous Silica SBA-15 Functionalized with High Concentration of Amino Groups Accessible to Metal Ions

WEI Qi[1*,1] ZHONG Zhen-Xing[1] NIE Zuo-Ren[1] CHEN Hui-Qiao[1] LI Qun-Yan[1] LI Cong-Ju[2]
([1]*College of Materials Science and Engineering, Beijing University of Technology, 100 Pingleyuan, Chaoyang District, Beijing*)
([2]*Beijing Key Laboratory of Clothing Material R&D and Assessment, Beijing Institute of Clothing Technology, Beijing* 100029)

Abstract: A facile strategy was used to synthesize highly ordered mesoporous silica SBA-15 functionalized with high concentration of amino groups, which seems to be rather difficult to be incorporated into mesoporous silica without disrupting the ordered mesoscopic structure compared to other functional groups. The pore structure of functionalized materials, together with the presence and accessibility of functional groups, were investigated in detail. It is shown that amino groups are attached covalently to the pore wall of SBA-15 and the ordered mesoscopic architecture of the functionalized samples remains almost intact even with a large concentration of aminopropyltriethoxysilane (APTES) up to 30mol% in the initial synthetic mixture. The samples with 20mol% APTES in the initial reaction mixture still preserve a desirable pore structure, with a surface area of 680 $m^2 \cdot g^{-1}$ and a pore volume of 0.89 $cm^3 \cdot g^{-1}$. Furthermore, the functional groups in such a porous structure are readily accessible and show a large affinity for nickel(Ⅱ) ion, with a Ni^{2+} adsorption capacity of 1.88 $mmol \cdot g^{-1}$, whereas no Ni^{2+} adsorption takes place with unfunctionalized mesoporous silica. The amount of amino groups incorporated increase as the APTES concentration further increases to 30mol%, but the amino groups are less accessible due to the dramatic decrease in the porosity of functionalized samples.

Key words: amino groups; mesoscopic order; pore structure; sccessibility; metal ion adsorption

收稿日期:2007-08-27。收修改稿日期:2007-11-22。
国家自然科学基金(No.50525413,50502002,50503001)和北京市教委科技计划(No.KM200610005016)资助项目。
*通讯联系人。E-mail:qiwei@bjut.edu.cn;Tel:010-67396206
第一作者:韦 奇,男,37 岁,博士,副教授;研究方向:多孔材料与无机膜材料。

Functionalization of mesoporous materials with organic functional groups has received considerable attention because functionalized mesoporous materials possess the mechanical properties of the rigid inorganic solid and the chemical reactivity of the organic moieties. Such inorganic-organic hybrid material may play an important role in many applications such as immobilization of enzymes and other biomolecules [1], high catalytic activity and selectivity [2~6], sensor design [7~8], drug delivery [9] and ion exchange due to their specific attributes such as binding sites, stereochemical configuration, charge density, and acidity [10]. Functionalization can be achieved by two approaches, i.e. post-grafting and direct synthesis. In the former method, organic functional groups are covalently attached to the pore surface by the reaction of the surface silanol groups on as-prepared mesoporous materials with the suitable organosilanes bearing specific functional groups using an appropriate solvent under reflux conditions [11]. The direct synthesis, based on the co-condensation of a tetraalkoxysilane precursor, for example, tetraethyl orthosilicate (TEOS), and one (or more) organoalkoxysilane(s) in the presence of a surfactant template, leads to a more uniform mesostructure and a better control over the surface properties of the resultant materials, compared to the post-grafting method [12]. This method has been widely used to functionalize mesoporous materials with many functional groups including aliphatic hydrocarbon [13], thiol [14,15], phenyl [16,17], amine [12,18,19,20] and sulfonic ligand [21,22].

The mesoscopic order of porous materials is directly related to their ability to perform the desired function in a particular application [4]. From the viewpoint of the immobilization and encapsulation of large molecules, well ordered mesoporous materials with large pores are more desirable [23,24]. However, the presence of organosilane would be more or less disruptive to the mesoscopic order of the functionalized mesoporous materials. It is reported that there is a limit of about 25mol% loading of organic groups in the mesoporous silica before the mesoscopic order is lost [25]. This observation is especially pronounced for the SBA-15 materials functionalized with amino groups using aminopropyltriethoxysilane (APTES) as co-precursor. Such surface modification yields terminal amino groups, which have been found to be useful for covalent coupling of protein to the surface of silica materials and selective adsorption of heavy metal ions such as Zn^{2+}, Cr^{6+} and Ni^{2+} [11,26,27]. Zhao et al [19,20] reported that the presence of a low concentration of APTES (17mol%) in the initial mixture led to a material with only one very broad SAXS peak, indicating a strong disruptive effect of APTES on the formation of SBA-15 mesostructure under the experimental conditions. In their opinion, this observation is attributed to the protonation of APTES under the highly acidic conditions, which might have a strong influence on the self-assembly of polymer P123 and lead to local disruptions of the silicate framework. Additionally, amino groups are also reported to damage the mesoscopic order of DAM-1 materials as evidenced by the broadening of the (100) reflection peak and the disa-ppearance of the higher order reflections [28]. Periodic mesoporous organosilicas (PMOs) have been reported to be incorporated by 25mol% APTES in the synthetic mixture, but the secondary reflections in XRD patterns are not resolvable, indicating that the functionalized materials are not highly ordered [16]. Che et al. [29]claimed a preparation of well-ordered mesoporous materials by a novel anionic surfactant templating route using APTES as co-structure-directing agent, but the chemical molar ratio of APTES/(APTES+TEOS) in the reaction mixture, for the samples AMS-2 and AMS-4, was only 11.9% and 9.1%, respectively. Walcarius et al [19] claimed that structural collapse was especially observed for the amino groups modified materials via the post-grafting method because of the basic character of amino groups, which can be contributed to the local hydrolysis events in the presence of water molecules. In the previous work, we compared in detail the effects of synthesis paramet-ers including TEOS pre-hydrolysis, as well as the heating temperature and time, on the mesoscopic order and pore structure of the amino-functionalized SBA-15. However, the amount of functional groups incorporated into SBA-15 was limited to 10mol%, and we failed to incorporate higher loading of functional groups in the final products

due to the remarkably different hydrolysis rates between the matrix precursor (TEOS) and the organosilane (aminopropyltrimethoxysilane, APTMS). Furthermore, we have not yet investigated the accessibility of functional groups, on which the applications of functionalized materials depend [30]. In spite of recent work highlighting the amino-functionali-zed silicas, to the best of our knowledge there has been little work reported so far related to the applications of those materials.

The hydrolysis of APTES was reported to be more controllable than that of APTMS since ethoxy groups are hydrolyzed slower than methoxy groups [16]. In the present paper, APTES is used instead of APTMS as organosilane to functionalize SBA-15 and the TEOS pre-hydrolysis of 2 h is adopted. By a facile strategy, highly ordered mesoprous silica SBA-15 is fuctionalized with much higher loading of amino groups than that previously reported. The presence of amino groups on the mesoscopic order and pore structure of the final products, are discussed and the accessibility of functional groups and the application of the final products in metal ion removal are also studied in detail.

1 Experimental

1.1 Materials synthesis

The synthesis of functionalized SBA-15 material was performed according to the following procedure with a molar ratio of TEOS:APTES:Surfactant:HCl:H_2O of (1-x):x:0.017:5.854:162.681, where x ranges from 0 to 40%. Triblock copolymer Poly (ethylene glycol)-B-Poly(propylene glycol)-B-Poly(ethylene gylcol), referred to as P123 (Sigam-Aldrich), was used as surfactant template. A certain amount of P123 (4.872 g, 99.9%) was dissolved in a mixture of water (127 mL) and 2 mol·L^{-1} HCl (25.53 mL) solution with strong stirring at 40 ℃, and then TEOS (11.3 mL, 98%) was added dropwise into the mixture. After reaction for 2 h, a certain amount of APTES (1.386 to 8.249 mL, 95%) was introduced into the sol mixture followed by a vigorous stirring for another 22 h until a white precipitate occurred. The mixture was moved into Teflon-lined autoclave and aged at 100 ℃ for 24 h. The products were filtered and air-dried, followed by surfactant removal by Soxhlet extraction with ethanol for 24 h. The final materials were obtained after drying at 60 ℃ in atmosphere overnight. The pure SBA-15 and functionalized samples with different molar ratios of APTES in the initial synthetic mixture are denoted as APS0, APS10, APS20, APS30 and APS40, respectively.

1.2 Materials characterization

Powder XRD patterns were obtained on a Bruker D8/advance diffractometer using a high power Ni-filtered Cu $K\alpha$ radiation (λ =0.154 18 nm) source, a solid detector and a scintillation counter at 35 kV and 35 mA. A resolution of 0.02°, a scanning speed of 0.5°·min^{-1} and a range from 0.6° to 6° were used. The morphology of the samples was observed by transmission electron microscopy (TEM, JEOL JEM-2010) operating at 200 kV. The samples were dispersed in acetone until a suspension was obtained, and a drop of the suspension was deposited and dried on a Cu grid. A low exposure technique was used to reduce the effect of beam damage and sample drift. N_2 adsorption was measured with Micromeritics ASAP 2020 at −196 ℃. Before analysis, the samples were first degassed at 110 ℃ for 5 h. The surface area was calculated according to BET equation at the relative pressure ranging from 0.05 to 0.20 and the pore size distribution was obtained from the desorption branch of isotherms using BJH approach. The pore volume was obtained by the amount adsorbed at saturated pressure. Solid state ^{29}Si NMR measurement was performed on a Bruker AV300 spectrometer operating at a frequency of 59.62 MHz with the following experimental conditions: magic-angle spinning at 5 kHz; $\pi/2$ pulse, 7 μs; a repetition delay of 600 s; 200 scans. The chemical shift was referenced to tetramethylsilane. The elemental analysis was conducted on Elmentar Vario EL. The adsorption behavior of Ni^{2+} for functionalized samples was investigated as follows. A 100 mg portion of adsorbent was added to 50 mL of an aqueous solution of Ni^{2+}(0.085 4 mol·L^{-1}, pH value of 7.5). After stirring for a given time (to guarantee an adsorption equilibrium), the supernatant solution was separated by centrifugation and the residual concentration of Ni^{2+} was analyzed with an ultraviolet-visible (UV-Vis) spec-

trometer (Thermo Evolution 600). The Ni^{2+} adsorption capacity(Q) was calculated by the following formula:

$$Q = V(C_0 - C) / m$$

Where C_0 and C represent the initial and the residual concentration of Ni^{2+}, respectively. V is the solution volume and m is the mass of functionalized SBA-15 used.

2 Results and discussion

2.1 Mesoscopic order of the functionalized samples

Fig.1 shows the XRD patterns of the pure and functionalized SBA-15 materials. It can be seen from the figure that a sharp peak at 2θ of 0.8°, assigned to (100) diffraction, together with two additional well-resolved peaks at 1.2° to 1.5° indexed as (110) and (200) reflections, respectively, are observed for the pure SBA-15 samples(APS0). This indicates that the samples have a highly ordered hexagonal *P6mm* structure. Similar to SBA-15 materials, the samples with APTES concentration ranging from 10 to 30mol% exhibit a considerably sharp peak of (100) reflection at the same 2θ position as that of the pure silica SBA-15. The higher order reflections are also observed in the 2θ position from 1.2° to 1.5°, although the intensity of (110) reflections slightly decreases compared to that of the pure samples. These XRD patterns of functionalized materials also suggest a highly ordered, hexagonally arranged pore system, indicating that the samples remain intact after incorporation of APTES with a concentration in reaction mixture as large as 30mol%. Our result is quite different from the previous report[12], where SBA-15 materials completely lose structural order after functionalization with a rather low concentration of APTES (5mol% in reaction mixture), as evidenced by the considerable broadening of the (100) reflection peak and the disappearance of the higher order reflections in the XRD patterns. The highly ordered pore arrangement of the functionalized materials herein can also be confirmed in the TEM images as shown in Fig.2. It can be seen from the TEM images taken from the direction parallel to the pore channels that the pores are hexagonally arranged, independent of the concentration of APTES. The pore diameters determined at a rough estimate from the images are located in the range of 4 to 6 nm, in good agreement with those calculated from the N_2 desorption isotherms reported below. If the APTES content in reaction mixture is further increased to 40mol%, the sample does not display any reflections, presenting a striking contrast to the functionalized materials with lower content of APTES, indicating that APTES has completely disrupted the long range ordered structure of

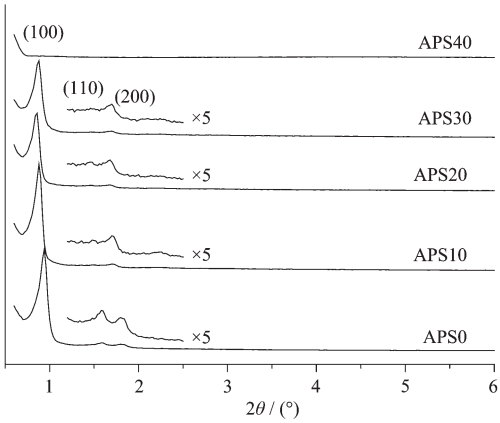

Fig.1 XRD spectra of the amino-functionalized SBA-15 with different molar concentrations of APTES in initial synthetic mixture. The region where (110) and (200) peaks appear is scaled 5 times

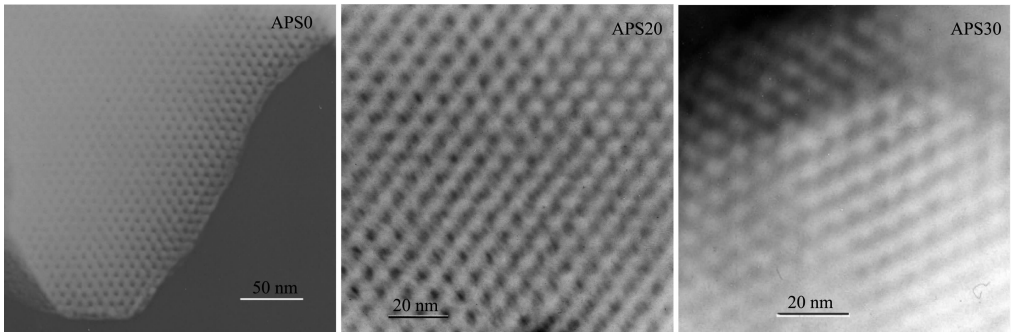

Fig.2 TEM images of the amino-functionalized SBA-15 with different molar concentrations of APTES in initial synthetic mixture, taken from the direction parallel to the pore channels

SBA-15 materials. Therefore, it can be inferred from Fig.1 and Fig.2 that at least 30mol% APTES in initial synthetic mixture, much higher than that reported previously, can be incorporated into the SBA-15 before the ordered structure is disrupted.

The above observation may be explained according to the following mechanism. In acid solutions, positive charge-bearing silicate species denoted as I^+ are produced through the hydrolysis of TEOS in terms of the following pathway[23]:

$$Si(OEt)_4 + nH_3O^+ \xrightarrow[pH<2]{\text{hydrolysis}} Si(OEt)_{4-n}\left(OH_2^+\right)_n + n\text{EtOH}$$

The EO moiety of P123 associates with hydronium ions as shown below.

$$REO_{m+y}HX \xrightarrow{H_2O} REO_{m-y}\left[\left(EO\cdot H_3O^+\right)\right]_y \cdots yX^-$$

Counterions (X^-=Cl^-) get involved as charge compensating species to keep the charge balance. The ordered mesostructure of SBA-15 is obtained through a so-called $(S^0H^+)(X^-I^+)$ pathway, where the surfactants and inorganic silicate species are assembled together by a combination of H-bonding, electrostatic, and van der Waals interactions[23]. If APTES is added into the mixture at the same time with TEOS, two kinds of reaction may occur in addition to the hydrolysis of TEOS and APTES and the charge associating of surfactants. On the one hand, amino groups of APTES is protonated in acid medium:

$$\equiv Si(CH_2)_3NH_2 + HCl \rightarrow Si(CH_2)_3NH_3^+ \cdots Cl^-$$

On the other hand, amine functions are known to interact strongly with silanol groups (i.e., via acid-base reactions [31]), leading to the formation of zwitterion-like species

$$\equiv Si(C_3H_6)NH_2 + HOSi\equiv \rightarrow \equiv Si(C_3H_6)NH_3^+ \cdots {}^-OSi\equiv$$

It can be seen that amino groups compete with silicate species and EO moieties of the surfactants for protons because the above four kinds of reaction occur at the same time. According to Zhao et al[12,20], the protonation of APTES and the formation of zwitterions are responsible for the disordered pore structures. However, a high ordered structure is observed if APTES is introduced two hour later, which might be due to the following factors. On the one hand, the hydrolysis of TEOS and charge associating of surfactants have consumed a large amount of protons in the solution, leading to a less pronounced protonation of APTES due to the decrease in proton concentration. On the other hand, polymerization of the TEOS has taken place and lasted for two hours via the condensation reaction between Si-OH species prior to the addition of APTES, inducing a considerable decease of residual surface silanol groups and therefore providing less opportunities to react with the "free" aminopropyl moieties to form the so-called zwitterions. The decease of protonated APTES and zwitterion concentration favors the formation of stable interface between P123 and silicate species. Furthermore, the interactions between protonated Si-OH moieties and charge-associated PEO units have lasted for enough long time to form a stable inorganic-organic hybrid interface, on which APTES added two hours later has a less adverse effect.

2.2 Pore structure of the functionalized samples

Fig.3 shows the N_2 adsorption-desorption isotherms of the functionalized samples. All the isotherms, with a clear hysteresis loop, can be classified as type Ⅳ, indicating the presence of mesopores. The result is quite different from the previous report, in which the sample with a APTES concentration of 9mol% displayed type Ⅰ isotherm of a microporous material instead of type Ⅳ[12]. With increasing in APTES concentration, the amount of N_2 adsorbed decreases and the capillary condensation occurs at lower relative pressure,

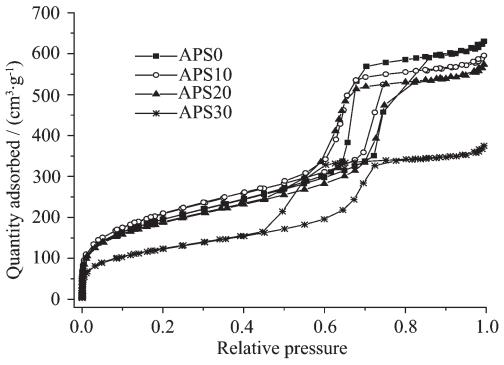

Fig.3 Isotherms of the amino-functionalized SBA-15 with different molar concentrations of APTES in initial synthetic mixture

demonstrating the decrease of both the porosity and pore size of the samples. The BJH pore size distribution curves computed from the desorption branch of the isotherms are shown in Fig.4 and the structure parameters are included in Table 1. All the samples display a narrow pore size distribution with a peak centered at 6.5, 5.6, 5.4 and 3.9 nm, respectively, as the APTES concentration increases from 0 to 30mol%. Both specific surface area and pore volume decrease upon modification, due to the space occupied by the aminopropyl chains bound on the inner surface of the mesopores. It is of great significance since the mesoporous architecture of the samples functionalized with a large amount of APTES remains desirable, with a surface area of 680 $m^2 \cdot g^{-1}$ and a pore volume of 0.89 $cm^3 \cdot g^{-1}$ even for the samples functionlized with 20mol% APTES in initial reaction mixture, without pronounced change compared to those of pure SBA-15 materials. The silica wall thickness increases from 4.4 to 7.7 nm, indicating that the amino groups are attached to the pore surface.

Table 1　Structure data of the amino-functionalized SBA-15 materials

Samples	Surface area / ($m^2 \cdot g^{-1}$)	Pore volume / ($cm^3 \cdot g^{-1}$)	PSD peak position / nm	d_{100} / nm	Wall thickness / nm
APS0	734	1.11	6.5	9.4	4.4
APS10	701	0.92	5.6	10.0	6.0
APS20	680	0.89	5.4	10.3	6.5
APS30	447	0.58	3.9	10.0	7.7

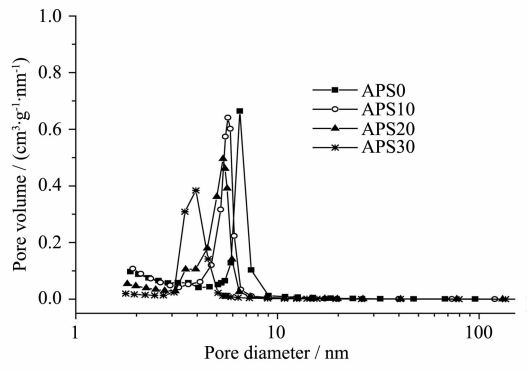

Fig.4　Pore size distribution of the amino-functionalized SBA-15 with different molar concentrations of APTES in initial synthetic mixture

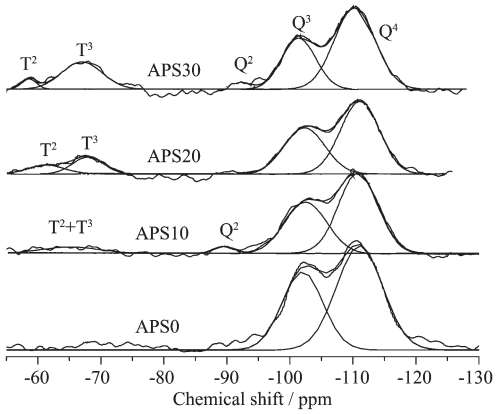

Fig.5　Solid state ^{29}Si MAS NMR spectra of the amino-functionalized SBA-15 with different molar concentrations of APTES in initial synthetic mixture. The spectra have been deconvoluted by Gaussian fit

2.3　Evidences for the presence of amino groups in functionalized silica

The extent of APTES incorporated into the mesostructured SBA-15 materials can be monitored by means of ^{29}Si MAS NMR, as shown in Fig.5. Only peaks at a chemical shift from −110 to −90 ppm, attributed to Q^4 [Si $(OSi)_4$],Q^3 [Si $(OSi)_3$ (OH)] and Q^2 [Si $(OSi)_2$ $(OH)_2$] silicon atom, respectively, are recorded for the pure SBA-15 materials (APS0). In addition to these signals, two additional resonances can be observed for organosiloxane [T_m=RSi$(OSi)_m(OH)_{3-m}$, m=1~3, and R=$C_3H_7NH_2$; T_3 at −66 ppm and T_2 at −60 ppm] species in the case of functionalized materials. The spectra can be deconvoluted according to Gaussian fit, in order to obtain the relative peak area of Q^m and T^m species (Table 2). From these data, the degree of amino groups incorporated [NH_2] per gram of functionalized materials (mmol $\cdot g^{-1}$) can be obtained. It can be seen from table 2 that the intensity of T^m signals increases gradually with increasing amount of APTES incorporated and the amount of amino groups reaches 2.68 mmol $\cdot g^{-1}$ for the functionalized material with APTES concentration of 30%, indicating that amino groups have been covalently attached to the pore surface of SBA-15 material. It can also be found that the final products all contain fewer

amount of functional groups compared to the concentration of organosilane in the initial synthetic mixture (for the sample APS20, $T^2+T^3=15.4$mol% <20mol%). Such observation is also found in the work of Markowitz and Mann groups, respectively [16,32]. The predominant reason for this might be the different hydrolysis rates between the matrix precursor and the functional silanes. One fraction of organosilane is not incorporated into the matrix when the TEOS condenses around the P123 assemblies during the formation of the ordered mesoscopic composite materials, and would then be removed away during the surfactant extraction step, if the rate of hydrolysis of the organosilane is not nearly the same as that of TEOS. The presence of functional groups in the final products is also confirmed by the elemental analysis of nitrogen, which is expected to derive from amino groups, as shown in Table 2. The amount of amino groups in the final products calculated from nitrogen content is slightly less than that determined from ^{29}Si MAS NMR, which might be attributable to the residual surfactant not completely removed by ethanol-extraction.

Table 2 Structure and property of the amino-functionalized SBA-15 materials

Samples	N / wt%[a]	NH_2 content / (mmol·g^{-1})[a]	Q^4 / mol%	Q^3 / mol%	Q^2 / mol%	T^3 / mol%	T^2 / mol%	NH_2 content / (mmol·g^{-1})[b]	Ni^{2+} adsorption capacity / (mmol·g^{-1})
APS0	—	—	59.45	40.55	—	—	—	0	0
APS10	1.21	0.86	53.86	37.22	2.37	3.18	3.37	0.97	0.80
APS20	2.62	1.87	50.5	34.1	—	9.5	5.9	2.16	1.88
APS30	3.04	2.17	51.59	27.03	1.91	17.13	2.34	2.68	0.84

[a] determined from elemental analysis

[b] calculated based on solid state ^{29}Si MAS NMR.

2.4 Accessibility of amino groups

The above discussion does demonstrate that amino groups have been incorporated into the final products, but it does not assure the accessibility of the amino groups. It is still uncertain that as the amount of incorporated amino groups increases, whether a corresponding increase in the amount of amino groups accessible for functionalization or as binding sites is observed or it plateaus at some lower level of amino incorporation. However, in a real application such as sorbent, catalysis or sensor, the functional groups need to be readily accessible for further reactions. In an attempt to understand the accessibility of the amino groups, adsorption of nickel(Ⅱ) from aqueous solution (pH value of 7.5) by amino-functionalized SBA-15 was studied at room temperature. It is found from Table 2 that pure SBA-15(APS0) shows no adsorption ability for Ni^{2+}[11], whereas functionalized samples are effective in Ni^{2+} adsorption. The sample APS20 possesses a Ni^{2+} adsorption capacity of 1.88 mmol·g^{-1}, much larger than that previously reported (1.02 mmol·g^{-1})[11], and also shows a superior adsorption performance to APS10 because it provides more amino groups. On the basis that a large excess of Ni^{2+} is present in the solution and assuming that one amino group will chelate one Ni^{2+} ion, it can be seen from Table 2 that most amount of amino groups in the sample APS20 and APS10 are accessible to Ni^{2+} since their Ni^{2+} adsorption capacity is nearly equal to the amount of amino groups in the final products determined from elemental analysis or ^{29}Si MAS NMR. Fig.6 shows the time course of the concentration of Ni^{2+} during the adsorption for the sample APS20. It is interesting that the sample adsorbs the same amount of Ni^{2+} in the first 240 min as it does in 1 200 min, indicating that equilibration takes place in

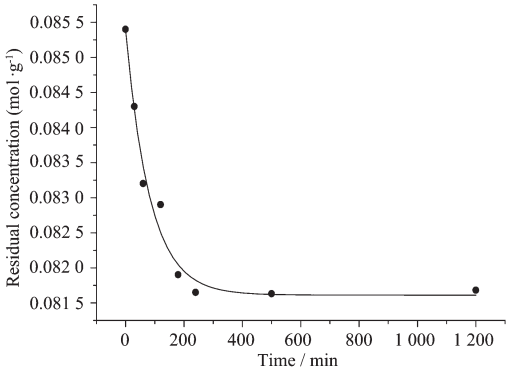

Fig.6 Time courses of concentration of Ni^{2+} in aqueous solution treated by the APS20 adsorbent

less than 240 min. However, as the concentration of APTES in initial mixture further increases to 30%, a dramatic decrease of Ni^{2+} adsorption is observed. This reveals that some amino groups are not accessible due to the sharp decrease of porosity, and thus providing fewer openings to the mesopore channels that are exposed to the Ni^{2+} solution.

3 Conclusion

Allowing tetraethoxysilane (TEOS) to hydrolyze for two hours prior to the co-condensation of TEOS and aminopropyltriethoxysilane (APTES) in the presence of triblock copolymer Poly (ethylene glycol)-B-Poly (propylene glycol)-B-Poly(ethylene gylcol)(P123) under acidic synthetic conditions, a large amount of amino groups are incorporated into mesoporous SBA-15 materials without disrupting their mesoscopic order. The samples with 20% APTES concentration in initial reaction mixture still preserve a desirable pore structure, with a surface area of 680 $m^2 \cdot g^{-1}$ and a pore volume of 0.89 $cm^3 \cdot g^{-1}$. Furthermore, the functional groups in such a porous structure are readily accessible and show large affinity for nickel(Ⅱ) ion, with a Ni^{2+} adsorption capacity of 1.88 $mmol \cdot g^{-1}$, whereas no Ni^{2+} adsorption take place with unfunctionalized mesoporous silica. The amount of amino groups incorporated into the final products increases with the concentration of APTES in the initial mixture, but they are less accessible due to the dramatic decrease of porosity for the sample APS30.

Acknowledgements: The financial support of National Natural Science Foundation of China (Nos.50525413, 50502002 and 50503001) and Scientific Research Common Program of Beijing Municipal Commission of Education (No.KM2006 10005016) are gratefully acknowledged.

References:

[1] Yan A X, Li X W, Ye Y H. *Appl. Biochem. Biotechnol.*, **2002**,**101**(18):113~130

[2] Brunel D, Blanc A C, Galarneau A, et al. *Catal. Today*, **2002**, **73**(1-2):139~152

[3] Stein A. *Adv. Mater.*, **2003**,**15**(10):763~775

[4] Davis M E. *Nature*, **2002**,**417**:813~821

[5] Soler-Illia G. J. de A. A, Sanchez C, Lebeau B, et al. *Chem. Rev.*, **2002**,**102**(11):4093~4138

[6] Ying J Y, Mehnert C P, Wong M. *S. Angew. Chem.*, **1999**,**38**(3): 56~77

[7] Lin V S-Y, Lai C-Y, Huang J, et al. *J. Am. Chem. Soc.*, **2001**, **123**(46):11510~11511

[8] Burleigh M C, Dai S, Hagaman E W, et al. *Chem. Mater.*, **2001**, **13**(8):2537~2546

[9] Lai C Y, Trewyn B G, Jeftinija D M, et al. *J. Am. Chem. Soc.*, **2003**,**125**(15): 4451~4459

[10]Vinu A, Hossain K Z, Ariga K. *J. Nanoscience & Nanotechnology*, **2005**,**5**(6):347~375

[11]Liu A M, Hidajat K, Kawi S, et al. *Chem. Commun.*, **2000** (13):1145~1146

[12]Maris Chong A S, Zhao X S, Kustedjo A T, et al. *Micropor. Mesopor. Mater.*, **2004**,**72**(1-3):33~42

[13]Mercier L, Pinnavaia T. *J. Chem.Mater.*, **2000**,**12**(1):188~196

[14]Beaudet L, Hossain K Z, Mercier L. *Chem.Mater.*, **2003**,**15**(1): 327~334

[15]Wei Q, Nie Z R, Hao Y L, et al. *Mater. Lett.*, **2005**,**59**(13): 3611~3615

[16]Burleigh M C, Markowitz M A, Spector M S, et al. *J. Phys. Chem. B*, **2001**,**105**(41):9935~9942

[17]Hall S R, Davis S A, Mann S. *Langmuir*, **2000**,**16**(3): 1454~1456

[18]Huh S, Wiench J W, Yoo J C, et al. *Chem. Mater.*, **2003**,**15** (22):4247~4256

[19]Walcarius A, Etienne M, Lebeau B. *Chem. Mater.*, **2003**,**15** (11):2161~2173

[20]Maria Chong A S, Zhao X S. *J. Phys. Chem. B*, **2003**,**107**(46): 12650~12657

[21]Melero J A, Stucky G D, Grieken R, et al. *J. Mater. Chem.*, **2002**,**12**(11):1664~1670

[22]Shen J G C, Herman R G, Klier K. J. Phys. Chem. B, **2002**, **106**(39):9975~9978

[23]Zhao D, Huo Q, Feng J, et al. *J. Am. Chem. Soc.*, **1998**,**120** (24):6024~6036

[24]Zhao D, Feng J, Huo Q, et al. *Science*, **1998**,**279**:548~552

[25]Asefa T, MacLachlan M J, Coombs N, et al. *Nature*, **1999**,**402**: 867~871

[26]Gass T F, Ligler S. *Immobilized Biomolecules in AnalysisA Practical Approach*. New York: Oxford University Press, **1998**.136

[27]Subramanian A, Kennel S J, Oden P I, et al. *Enzyme Microb. Technol.*, **1999**,**24**(1-2):26~34

[28]Coutinho D, Madhugiri S, Balkus K J, et al. *J. Porous. Mater.*, **2004**,**11**(3):239~254

[29]Che S, Bennett A E G, Yokoi T, et al. *Nature Mater.*, **2003**,**2**: 801~805

[30]Wei Q, Nie Z R, Hao Y L, et al. *J. Sol-Gel Sci. Technol.*, **2006**,**39**(2):103~109

[31]Despas C, Walcarius A, Bessiere J. *Langmuir*, **1999**,**15**(9): 3186~3196

[32]Fowler C E, Burkett S L, Stephen Mann S. *Chem. Commun.*, **1997**(18):1769~1770